Exploring the Potential of EnMAP Hyperspectral Data for Crop Classification: Technique and Performance Evaluation

Jonali Goswami[1], Ovungrhoni V. Murry[1], Prasanna Boruah[2], S.P. Aggarwal[1]

[1]North Eastern Space Applications centre, Umiam, Meghalaya jonali.goswami@gmail.com, ovungrhonivmurry1@gmail.com, director@nesac.gov.in
[2]Assam State Space Application Centre, Guwahati, Assam pboruah.21@gmail.com

Keywords: Hyperspectral remote sensing, spectral library, EnMAP, agriculture, Crop Classification, accuracy assessment

Abstract

Hyperspectral remote sensing is one powerful component that contributes to precision agriculture. The study explores the potential of EnMAP hyperspectral data for the classification of crop types in Goroimari, Kamrup, Assam. The targeted crops namely Sali rice, Rabi maize, mustard and potato are the major Kharif crops grown in the area. A standard protocol for spectra and metadata collection was prepared to be followed while collecting the field spectra. A spectral library of the crops is prepared by collecting spectra in the field using SVC HR-1024 spectroradiometer. After preparing the spectral library as a reference for identification, EnMAP hyperspectral data of the study area, acquired at a similar time with the field data collection is obtained. Utilizing the high spectral resolution of EnMAP with ground field spectra of targeted crops, a combination of end member extraction, endmember spectral matching and Spectral Angle Mapper (SAM) algorithm was implemented to effectively differentiate between various crop types. Three additional classes were identified i.e., crop residue, fallow and sandbar class. The identified endmember classes were taken as the reference spectra to classify the area using SAM. An overall classification accuracy of 88.43 % was achieved. The study demonstrates the potential of EnMAP hyperspectral data in discriminating crop type.

1. Introduction

The pressure on agriculture continues to grow with increasing population. Managing agriculture resources and attaining food sustainability is one of the greatest challenges that humanity faces today. Improved productivity with the use of optimum resources and reduced stress on the environment has become the major goal of all economies. Precision agriculture has paved the way for an improved and modernized management of agriculture. Hyperspectral remote sensing is one powerful component that contributes to precision agriculture including discerning different crop types or species (Sahoo et al., 2015), study of biochemical composition (Haboudane et al., 2022; Kanan et al., 2023), physical structure, water and nutrient content, plant eco-physical status (Strachan et al., 2002), crop monitoring, disease and stress study and yield (Jin et al., 2016) and acreage estimation. The technology has found application in numerous fields owing to the rich spectra generally ranging between 350 nm to 2500 nm. The narrowness of the wavelengths and the big number of bands provides greater details and information, which are otherwise hard to obtain via broad band remote sensing. However, the complexity and efficiency of hyperspectral remote sensing data analysis are constrained by the lack of suitable methodologies. Even though there has been substantial advancement in data dimensionality reduction and the correlation of hyperspectral data with material type, the research field of remote sensing continues to be hindered by the large volume of hyperspectral cube. In agriculture applications there is also the restrain of hyperspectral data availability and a spectral library for reference. Nevertheless, the identification of objects based on their unique spectra has improved any type of spatial classification.

The advent of recent European Space Agency's Environmental Mapping and Analysis Program (EnMAP) has revolutionized environment monitoring with the availability of free hyperspectral data. Launched in April 2022, it was the first hyperspectral satellite developed and built in Germany. The purpose of the EnMAP mission is to provide high quality regional hyperspectral measurements for application in agriculture and forestry, ecosystem compositions and dynamics, geology and soils, coastal studies, hydrology and cryosphere studies (EnMAP, 2022). In hyperspectral data analysis, spectral library is a prerequisite as object identification can be done only if a known reference spectra is available. Spectral libraries assemble spectra that have been acquired either in the laboratory or in the field using Spectroradiometer (Manjunath et al., 2014). Developing a spectral library is a key component to improve the capacity in utilizing the full mapping potential from data provided by airborne and advanced space-borne hyperspectral images (Zomer et al., 2009). A ground based hyperspectral analysis has been carried out by (Sowmya et al., 2014) to acquire the spectral signatures using ASD for the crops like chick pea, cow pea, cotton, groundnut, rice, black gram and also for the soil in the field. A study has also been carried out to gather spectral data and related background characteristics for various crop growth periods in South China (Chen et al., 2005). There are various challenges and numerous parameters to consider while developing a spectral library for crops owing to its differences in reflectance spectra due to variations in the phenological stages, crop cultivar, soil and weather variations (Andries et al., 2021). Hence, an ancillary data is an essential component while preparing a spectral library as it contains information on the quality, completeness, and utility of the spectral data acquisitions (Dela Torre et al., 2016).

With the availability of good spectral library with detailed ancillary data, identification of objects on the earth's surface becomes easier. Spectral Angle Mapper is a time-tested classification method which evaluates the spectral similarity with the endmembers or spectral library by calculating the angle between pixel spectra and reference spectra in n-dimensional space (Kruse et al., 1993). The algorithm does not address the problem of mixed spectra of heterogeneous earth's surface. Nevertheless, it has proven to give favourable results like the study done by (Girouard et al., 2004) have used SAM for mineral mapping. Numerous other studies like (Richardson and Kruse, 1998) and (Bogliolo et al., 1998) also used it for spectral analysis.

The study aims to explore the potential of EnMAP hyperspectral data in crop classification, which is one of the first studies to our knowledge. Additionally, a standard procedure for field spectral data collection is highlighted in this study. Following the standard format, the authors aim to develop a spectral library specific to the region for the targeted crops namely Sali rice, Rabi maize, Mustard and Potato. The study area consists of an agricultural landscape in Goroimari, Kamrup, Assam. In this study, heuristic endmember extraction method was implemented using Pixel Purity Index (PPI) (Boardman et al., 1995) to extract the spectrally pure pixels from the image. The pure pixels are matched with the spectral library to assign a class and the image is classified using SAM classification algorithm. The overall goal is to test the capabilities of EnMAP hyperspectral data for crop identification using the reference spectral library developed for this purpose.

2. Study area

The given Figure 1 depicts the study area shown by LISS-IV data having a total geographical area of 55.210 Km^2. Out of which a total of 24.701 Km^2 area is under agriculture. The study area consists of a part of Goroimari block, situated at Kamrup district of Assam. It is located at 26°6'52.6032" North latitude and 91°14'34.1736" East longitude at an elevation of 140 m above mean sea level. The region has a subtropical humid climate with high humidity, scorching summers, and substantial summer rainfall. The annual average temperature ranges from 12 to 38 °C. According to IMD data, the district typically receives 2125.4 mm of precipitation per year with 96.5 rainy days. The population is dependent on agriculture.

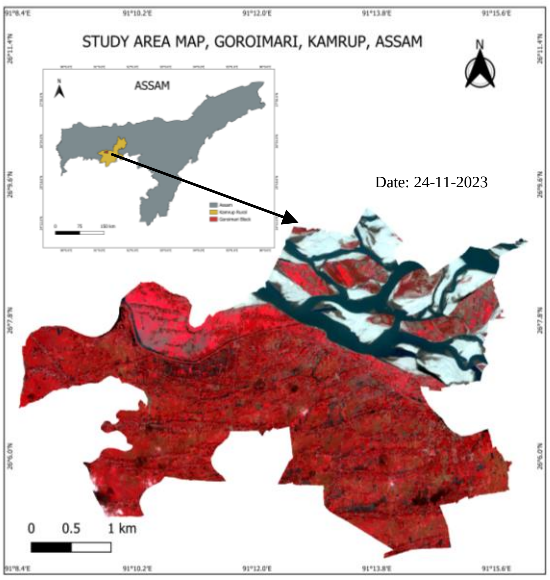

Figure 1. Study area map of Goroimari, Kamrup, Assam.

3. Methodology and data used

3.1 Spectral data collection

A standard protocol for spectral and metadata collection specifically for crops was generated as per the guidelines of Science Plan and Implementation Strategy, NISA (Ramakrishnan and Sahoo, 2016). A detailed ancillary data are recorded while taking the field data for better interpretation (Campbell and Wynne, 1996). The field spectral measurements were carried out using the SVC HR-1024 field portable Spectroradiometer from the Spectra Vista Corp (SVC). It has a wavelength range between 350-2500nm which covers UV, Visible and NIR region, with varying bandwidth of minimum 1.5 nm in the visible to 3.8 nm in the SWIR region with a total of 1024 spectral bands (SVC 2019). A PC-assisted operation for data collection was carried out using the SVC HR-1024 PC Data Acquisition Software. This computer based operation allows easy real time display and analysis of data. Dark measurement was set to 'auto dark' mode. 'Freshly' calibrated white reference reflectance panel made up of PTFE (Polytetrafluoroethylene) tile was used for reference scan. Spectroradiometer is also calibrated with each Foreoptic lens for spectral radiance and with the integrating sphere for spectral irradiance. The observation window was strictly kept between 11:00 to 13:00 h when the sun is almost overhead. The crop spectra were collected between November and December, 2023 and a minimum of 5 readings were taken for each crop. The final spectra were selected based on the first derivative of each spectrum and by visual inspection for any erroneous values.

3.2 Spectral data processing

The step involves removal of overlapped spectral data, deriving spectral reflectance, smoothening of spectra and water band removal (Robinson, 2024). First derivative of the smoothed spectra is additionally inculcated to study the absorption points of the crop. The spectral processing was done using python in Visual Studio Code (Version 1.86). A flow chart of the spectral data processing is given below (Figure 2).

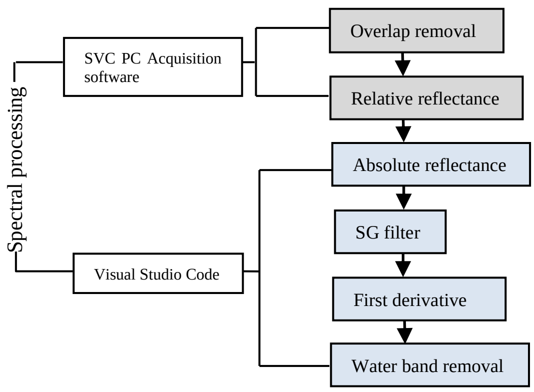

Figure 2. Flow chart of spectral data processing methodology.

3.2.1 Overlap removal: There is a spectral overlap area towards the VNIR and SWIR region between 960 nm to 1000 nm (Figure 3). Most spectroradiometers have multiple detectors to cover the spectral regions of VNIR and SWIR which causes an overlap. This overlap data needs to be removed for further processing. In the SVC PC acquisition software, there is a setting to remove or retain the overlap regions automatically when the data is taken. The SIG file overlap/matching tool in the software can also be used to remove overlap regions.

https://doi.org/10.5194/isprs-annals-X-G-2025-291-2025

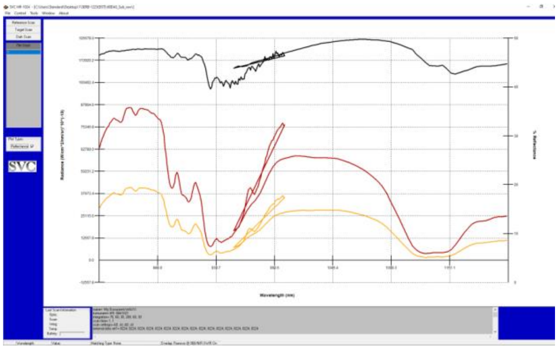

Figure 3. Spectral overlap in the region between 960 and 1000 nm as seen from the SVC PC acquisition software.

3.2.2 Relative reflectance: Relative reflectance (R_{rel} (λ)) is calculated as the ratio of reflected light measured from the target (L (λ)) to the amount of reflected light measured from the reference panel (E_{rel} (λ)) in their respective wavelengths. Here the reference plate is assumed to have a reflectance of 100%. It is simply the ratio of target spectrum to the reference spectrum (Robinson and Arthur, 2011)

$$\mathbf{R_{rel}}\ (\boldsymbol{\lambda}) = \frac{\mathbf{L}\ (\boldsymbol{\lambda})}{E_{rel}\ (\lambda)} \quad (1)$$

3.2.3 Absolute reflectance: Absolute reflectance is calculated using the relative reflectance (R_{rel} (λ)) by multiplying it with a reference panel calibration spectrum (R_{panel} (λ)). The panel calibration file can be found in comma-separated values (csv) or an excel spreadsheet which has a record of the panel reflectance over a set of wavelengths. The wavelengths of the panel calibration file are interpolated to match the wavelengths of the relative reflectance. (Robinson and Arthur, 2011)

$$\mathbf{R_{abs}}\ (\boldsymbol{\lambda}) = \frac{R_{panel}(\lambda)}{R_{rel}(\lambda)} \quad (2)$$

3.2.4 Savitsky-Golay smoothening: Smoothening of spectra is mandatory to produce meaningful spectral derivatives. One of the most used smoothening techniques i.e., Savitsky-Golay (SG) filter (Savitsky and Golay, 1964) is applied to the Absolute reflectance spectra to reduce noise and smoothen the spectral signature. The smoothed spectra will have a new range of wavelengths.

3.2.5 First derivative: A first derivative of spectra is obtained using the smoothed spectra. The first derivative of spectra shows the rate of change of absorbance with respect to wavelengths. It starts and ends at zero at the wavelength where absorbance is the maximum (Owen, 2000). The first derivative spectra can be used to analyze the absorption points of different crops.

Water band removal: Strong water absorption occurs in the wavelength ranging from 1350 nm to 1460 nm and from 1790 to 1960 nm. The spectra in the water absorption bands are erratic and noisy. Water band removed spectra is obtained by removing the values within these ranges from the smoothed spectra.

3.3 Classification:

The specification of EnMAP sensor is given in Table 1. It has a daily spatial coverage of 30 km × 5000 km and a ground sampling distance (GSD) of 30 m x 30 m. With the use of two different spectrometers, it can measure a wavelength in more than 240 consecutive bands in the visible to near-infrared (VNIR) and short-wave infrared (SWIR) spectral range from 420 to 2450 nm. EnMAP hyperspectral data of Processing Level 2A (L2A) which is atmospherically corrected and orthorectified, acquired on 28 November 2023 is obtained for the study area.

Hyperspectral cubes contain bad bands which consist of low signal to noise ratio or no data at all. These bands need to be removed before further processing to avoid discrepancies in analysis and classifications. Agriculture area layer was overlaid on the hyperspectral data. Utilizing the high spectral resolution of EnMAP with ground field spectra of targeted crops (Sali rice, Potato, Rabi maize and Mustard), SAM classification algorithm was utilized to effectively differentiate between various crop types. ENVI software is utilized for the processing of hyperspectral data.

Platform	**EnMAP**
Country	Germany
Organisation	GFZ-DLR
Sensor type	Hyperspectral
Ground Sampling distance (m)	30
Swath (Km)	30
No. of bands	246
Spectral range (nm)	420-2450
Spectral resolution	6.5 nm in VNIR 10 nm in SWIR
Radiometric resolution (bits)	14
Date of acquisition	28th November 2023

Table 1. EnMAP hyperspectral specifications.

3.3.1 Endmember extraction: The process begins with Minimum Noise Fraction (MNF) transformation which produces orthogonal components in the order of image quality as a function of signal to noise ratio (SNR). The first few components have high signal to noise ratio. Subsequent to the MNF transformation, the Pixel Purity Index (PPI) algorithm is employed to segregate the pure pixels from the MNF bands (Pargal, 2011; Piragnolo et al., 2021). The PPI algorithm makes an assumption that for each endmember, there exists, at least one pixel which belongs to that endmember only. A band threshold of the pure pixels are set and exported as region of interest pixels associated with the hyperspectral data. The pixels are plotted in the n-dimensional Visualizer to cluster the pixels of the same class.

3.3.2 Spectral matching: Further the spectral analyst tool was utilized to match the spectra of the unknown classes with the known spectra in the spectral library by ranking the match with the use of Binary Encoding (Mazer et al., 1988), Spectral Angle Mapper (SAM), and Spectral Feature Fitting (SFF). SFF compares the fit of image spectra to reference spectra using a least-squares technique and absorption-feature-based methodology. SAM compares the similarity of the spectra in radians and binary encoding compares the spectra in percentage of bands correctly matched. Equal weights were assigned for each similarity measurements. Along with this, ground truth information was integrated to validate the match. The spectral library was resampled to the same wavelength as the EnMAP data prior to spectral matching.

3.3.3 SAM classification: In addition to the identified crop spectra, three more classes were identified i.e., crop residue, fallow and sandbar class. The identified endmember classes were taken as the reference spectra to classify the area by employing Spectral Angle Mapper (SAM) algorithm. SAM classifies pixels based on their angle relative to the endmember spectrum, with smaller angles indicating closer matches. Pixels exceeding a specified maximum angle threshold are not classified (Kruse et al., 1993).

SAM is presented by the following formula (3):

$$\alpha = \cos^{-1}\frac{\sum XY}{\sqrt{\sum(X)^2\sum(Y)^2}} \tag{3}$$

Where, α = angle between reference and target spectrum
X= Target spectra, Y= Reference spectra
A default standard threshold of 0.1 radians was used in this study. SAM classification uses the n-dimensional angle to match pixels with the endmember spectra. Here the dimensionality is equivalent to the number of bands. The smaller the angle, the closer is the match to the reference spectra. The minimum angle threshold is set and the pixels further away than the specified angle are not classified. An accuracy assessment of the classified image is done using confusion matrix with the ground truth points collected in the field.

4. Results and discussion

4.1 Spectral library

The spectral library consists of two main parts viz. crop spectra files and the associated metadata collected following the standard format given in Annexure-1 at the end of this document. The crop spectra files consist of the smoothed crop spectra, first derivative of the spectra and water band removed spectra.

The metadata comprises information pertaining to the field survey report. The whole process of data collection from the type of spectroradiometer used to the type of crops, number of attempts made, orientation of leaves while taking the spectra are recorded. Crop details like the variety name, Phenology, days after sowing or planting are also recorded in the metadata.
The record contains detailed information pertaining to the location of the field, date and time of where and when the data was acquired. It contains weather condition parameters like wind speed, temperature and sunlight. The photograph of the crops are given below in Figure 4.

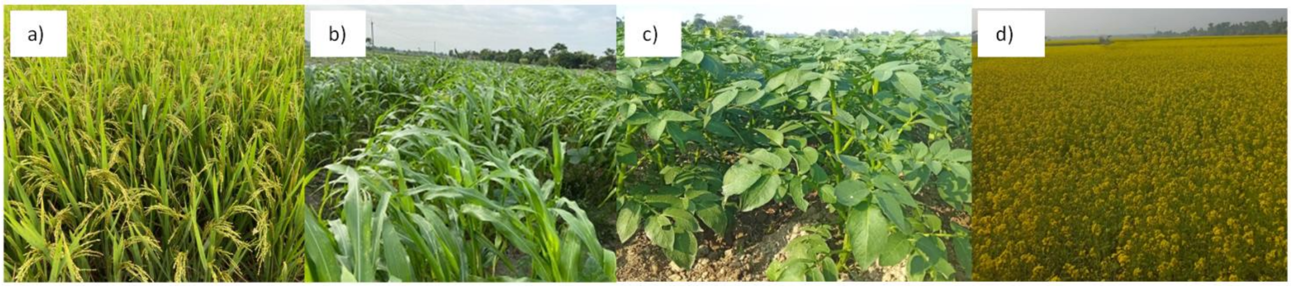

Figure 4. Field photographs of the crops taken during field data collection - a) Sali rice b) Rabi maize c) Potato d) Mustard.

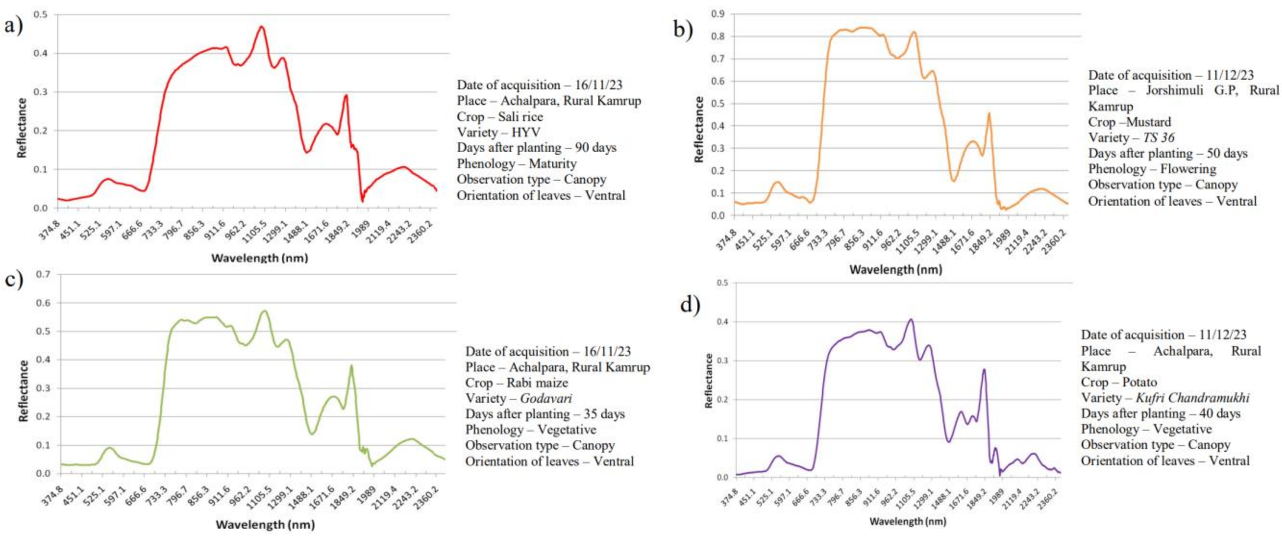

Figure 5. Smoothed spectra of each crop along with some metadata collected from the field - a) Sali rice b) Mustard c) Rabi maize d) Potato.

Figure 5 shows the smoothed spectra of Sali rice, Rabi maize, Mustard and Potato along with some metadata information. The X axis represents the wavelength in nanometers ranging from 350 to 2500 nm. And the Y axis shows the reflectance in percentage normalised from 0-1.

Rabi maize and potato spectra were taken during the vegetative stage. Sali rice and mustard were taken at matured and floweing stage respectively. In the visible range (400-700 nm), the spectral reflectance is comaparatively low due to the absorption by leaf pigments like chlorophyll, cartenoids, xanthophylls and polyphenols (Gitelson et al., 2001). In the near-infrared (NIR) region (700-1300 nm), the reflectance is high due to the internal cell structure and the leaf pigments and cellulose becomes transparent (Rouse et al., 1973). The red edge (680-750 nm) is found in this region which is the steep slope between the red and NIR range as we can observe from all the four crop spectra. This is also attributed to the chlorophyll pigments as it strongly absorbs blue and red light for photosynthesis. The Short Wave Infrared region (SWIR 1300-2500 nm) is dominated by water absorption region as we can deduce from the given crop spectra (Ustin et al., 1999).

Figure 6 shows the first-order derivative of the smoothed spectra. It represents the rate of change of absorbance respective to the wavelength. It passes through zero at the wavelength where the absorbance is maximum. The first derivative spectra was used to select the final spectra input for the spectral library. These spectra can be used as a standard reference in the future studies however this spectral library is limited only to those areas having similar agro climatic region as the study area. The spectra is also limited to the particular crop variety and the crop growth stage.

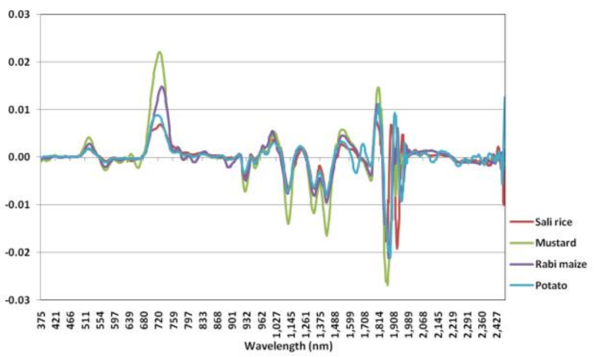

Figure 6. First order derivative spectra of the smoothed crop spectra.

4.2 Classification

After bad band removal from the EnMAP data, a total of 202 bands were utilised out of 246 for the classification ranging from 420 to 2450 nm. Using the MNF transformation, we obtained the first six bands which have the maximum SNR based on the Eigen value. After which the pure pixels are identified using PPI by analysing the distribution of pixels in the transformed space of the MNF bands. The extreme pixels in each projection are recorded and a pure pixel Image is created where each pixel value corresponds to the number of times that pixel was recorded as extreme. Based on the minimum and maximum values of the pure pixel analysis i.e., 1 and 6,991 respectively, a band threshold is set and exported. Using the n-dimensional Visualizer, a total number of 13 unknown cluster or classes of the pure pixels are obtained. Using the spectral analyst tool, the crop classes were identified using the spectral library namely Sali rice, Rabi maize, Mustard and Potato. Figure 7 shows the spectral match of the EnMAP spectra with the spectral library.

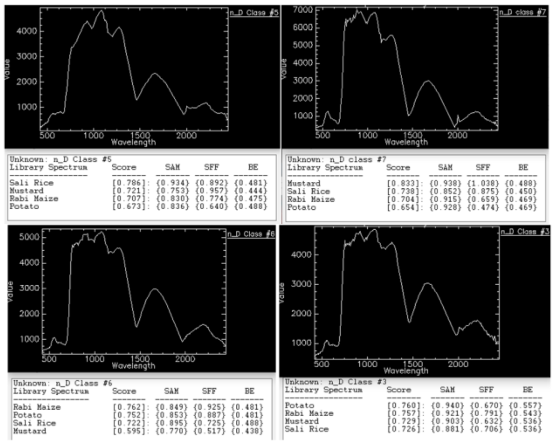

Figure 7. Spectral matching of unknown spectra with the known spectra using spectral analyst.

A total of seven classes were identified including the four crop classes and three additional classes. Crop residue, fallow and sandbar class were identified based on the spectra and spatial distribution. The spectral analyst tool does not identify the spectra directly but it only suggests the likely spectra that might be a match. The final matched spectra were validated with ancillary information. The average spectra of each identified classes are given in Figure 8. The remaining unknown classes were discarded. SAM classification is applied with the endmembers as the input spectra for reference. As a single endmember consists of numerous pixels, the algorithm takes an average of the spectra. Only the pixels matching with the endmember spectra having an angle less than 0.1 radians are classified as that particular class.

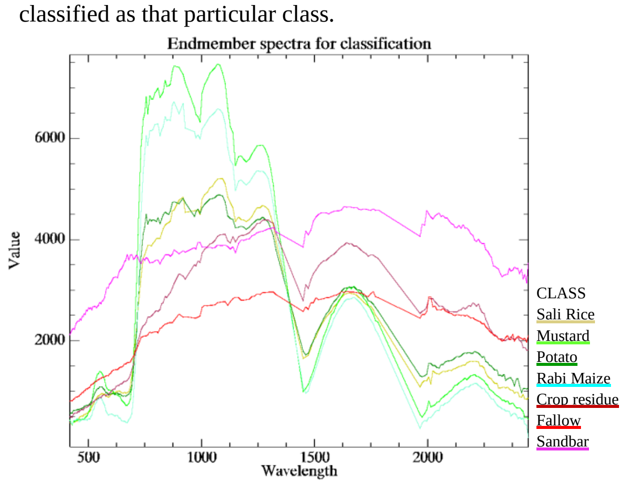

Figure 8. Spectra of the identified endmembers of EnMAP hyperspectral data.

The pixels that do not match any of the endmembers are not classified. The classified image is shown in figure 9. It represents the crop class map of the study area. Sali rice is majorly distributed over the western and eastern regions. Most of the crop residue pixels are attributed to rice crop residue as some plots have already been harvested at this time of the season. The Northern parts of the study area which are much closer to the river are covered with potato and mustard fields. Only a few maize fields were identified due to the field size. Most of the north eastern part of the study area which is a river island is fallow and the edges are covered by sandbar near the river. The classified output gives an overall idea about the distribution of crops in the study area. The method used in this study for crop classification using EnMAP hyperspectral data is validated through the achievement of good accuracy.

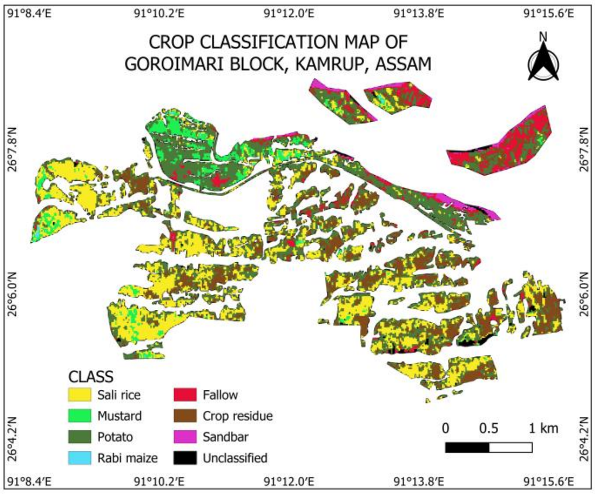

Figure 9. Crop classification map of Goroimari, Kamrup, Assam.

A total classification accuracy of 88.43 % was attained. Nevertheless, there are several restrictions that have a possible impact on the quality of the overall analysis. The main concern is the low spatial resolution of the hyperspectral data which is 30 m. A large number of agricultural fields are smaller than the pixel size and the occurrence of mixed pixels problem is very high. Due to this reason, it becomes challenging to classify crops accurately if the spectra of several objects are combined in a single pixel. Moreover, the study mostly focused on the selected crops that usually occupy larger fields, which could result in an underrepresentation of the variety of crops grown in the area. Furthermore, the ground truth points for accuracy assessment were taken such that the points are at 30 m away from each other considering the pixel size, which could not have been sufficient to fully reflect the heterogeneity found in smaller agricultural plots. Crop type mapping at small scales using space based hyperspectral sensors are hindered by the low spatial resolution due to the trade off in the spectral resolution. Future research can explore the domain of integrating hyperspectral data with multispectral data to achieve a combination of spectrally rich and higher spatial resolution. This could potentially improve crop identification at a small scale.

5. Conclusion

In this study, a crop classification map of Goroimari, Kamrup, Assam was successfully prepared using EnMAP hyperspectral data with a classification accuracy of 88.43 %. An overall methodology for spectral library-based crop classification using SAM algorithm is highlighted in this study. A standard protocol for hyperspectral and metadata collection has been laid out in this study and it can be referred for field spectral data collection of agricultural crops. The spectral library can be utilized in the initial identification and mapping of the given crops namely Sali rice, Rabi maize, mustard and potato specific to the variety, phenology and region. It will serve as a basis for crop health monitoring, nutrient requirements, stress and disease detection, thereby improving crop management and better use of agricultural resources. The study successfully demonstrated the applicability of hyperspectral remote sensing data in crop identification and mapping. However, with the available spatial resolution (30m), the study is limited to the field size and homogeneity of the crops. With the availability of good resolution (temporal, spatial) hyperspectral data, spectral library and the integration of GIS tools, the agriculture sector can benefit greatly from this technology.

References

Boardman, J.W., Kruse, F.A., Green, R.O., 1995. Mapping target signatures via partial unmixing of AVIRIS data. *Summaries of the fifth annual JPL airborne earth science workshop*. Volume 1: AVIRIS workshop.

Bogliolo, M.P., Teggi, S., Buongiorno, M.F., Pugnaghi, S.,. 1998. Retrieving Ground Reflectance from MIVIS Data: A case study on Vulcano Island (Italy). 1*st EARSeL Workshop on Imaging Spectroscopy, Remote sensing Laboratories*, University of Zurich, Switzerland 403-416.

Campbell, J.B., Wynne, R.H., 1996. *Introductiuon to Remote Sensing.* New York: The Guilford Press.

Dela Torre, D.M.G., Pagkalinawan, H.M.,. Cruz, C.A., Crystal Grace P. Dimalanta , Gatdula, N.B., Eric Luis M. Tañada , Julius Caezar L. Aves , Mark Sueden Lyle Y. Magtalas , Geozza D. Tan , Ransie Joy A. Apura , Therese Anne M. Ro, 2016. Development of field sampling protocols for a spectral library. (Asian Assocoation on Remotesensing) 6.

EnMAP. *EnMAP*. https://www.enmap.org (accessed March 5, 2024).

Gazzea, M., … Arghandeh, R., 2022. Tree Species Classification Using High-Resolution Satellite Imagery and Weakly Supervised Learning. *IEEE Trans. Geosci. Remote Sensing* 60, 1–11.

Girouard, G., Bannari, A., Harti, A.E.,Desrochers, A., 2004. Validated spectral angle mapper algorithm for geological mapping: comparative study between QuickBird and Landsat-TM. January.

Gitelson, A.A., Merzlyak, M.N., Zur, Y., Stark, R., Gritz,U., 2001. Non-destructive and remote sensing techniques for estimation of vegetation status. *Third European Conference on Precision Agriculture* 301-306.

Haboudane, D., Miller, J.R., Tremblay, N., Zarco-Tejada,P.J., Dextraze, L., 2022. Integrated narrow-band vegetation indices for prediction of crop chlorophyll content for application to precision agriculture. *Elsevier* 416-426.

Jin, X., Kumar, L., Zhenhai, L., Xu, X., Yang,G., Wang, J., 2016. Estimation of Winter Wheat Biomass and Yield by Combining the AquaCrop Model and Field Hyperspectral Data. *Remote sensing*.

Kanan, A.H., ... Rahman, M.M., 2023. Mapping inundation from sea level rise and its interaction with land cover in the Sundarbans mangrove forest. *Climatic Change* 176, 104.

Kruse, F.A., Lefkoff, A.B., Boardman, J.W., Heidebrecht, K.B., Shapiro, A.T., Barloon, P.J., Goetz, A.F.H., 1993. The spectral image processing system (SIPS)—interactive visualization and analysis of imaging spectrometer data. *Remote Sensing of Environment* 44, no. 2-3 145-163.

Manjunath, K. R., KumaR, A., Meenakshi, M.,Renu, R., Uniyal, S. K.R., Singh, D., Ahuja, P. S., Ray, S. S., Panigrahy, S., 2014. Developing Spectral Library of Major Plant Species of Western Himalayas Using Ground Observations. *Springer Journal of the Indian Society of Remote Sensing* 201-216.

Mazer, A.S., M. Martin, M. Lee, and J.E. Solomon, 1988. Image Processing Software for Imaging Spectrometry Analysis. *Remote Sensing of the Environment* 24 201-210.

Owen, A.J. 2000. Uses of Derivative Spectroscopy Application Note UV-Visible Spectroscopy. *Agilent Technologies*.

Pargal, Sourabh, 2011. Hyperpsectarl Subspace Identification and Endmember Extraction by Intergration of Spatial-Spectral Information. The Netherlands: University of Twente AND Indian Institute of Remote Sensing.

Piragnolo, M., ... Grigolato, S., 2021. Responding to Large-Scale Forest Damage in an Alpine Environment with Remote Sensing, Machine Learning, and Web-GIS. *Remote Sensing* 13, 1541.

Ramakrishnan, D., Sahoo, R.N., 2016. Science Plan and Implementation Strategy Network program on Imaging Spectroscopy and Applications(NISA). New Delhi: Department of Science and Technology.

Richardson, L.L., Kruse, F. A., 1998. Identification and Classification of Mixed Phytoplankton..

Robinson, I., Arthur, A.M.,. 2011. Post processing field spectra in MATLAB. Field Spectroscopy Facility, Natural Environment Research Council,.

Robinson, Iain. 2024. Field Spectroscopy Facility Post Processing Toolbox , MATLAB Central File Exchange. (https://www.mathworks.com/matlabcentral/fileexchange/31547-field-spectroscopy-facility-post-processing-toolbox).

Rouse, J.W., Haas, R.H., Deering, D.W., Schell, J.A., & Harlan, J.C. 1973. Monitoring the Vernal Advancement and Retrogradation (Green Wave Effect) of Natural Vegetation. [Great Plains Corridor].

Sahoo, R. N., Ray, S. S., Manjunath, K. R., 2015. Hyperspectral remote sensing of agriculture. *Current Science* 12.

Savitzky, A., Golay,M. J. E., 1964. Soothing and Differentiation of Data by Simplified Least Squares Procedures. *Analytical Chemistry* 36: 1627-1639.

Sowmya, P., Giridhar, M.V.S.S., Prabakar, M.,. Development of Spectral Library for Different Crops using Spectroradiometer. *Proceedings of Two day National conference on Water, Environment and Society organized by CWR, JNTUH on June 30th – July 1st 2014.* BS Publications, 2014. 556-561.

Strachan, I.B., Pattey, E., Boisvert, J.B., 2002. Impact of nitrogen and environmental conditions on corn as detected by hyperspectral reflectance. *Remote Sensing of Environment* 213-224.

SVC. Field Spectroscopy Guide with SVC i-series Spectroradiometers. 22 October 2019.

Ustin, S. L., Roberts,D.A., Green, R.O.,Zomer, R.J., Garcia, M.,. Remote sensing mthods monitor natural resources. *Photon Spectra*, 1999: 108-113.

Zomer, R.J., Trabucco, A., Ustin, S.L.,. Building spectral libraries for wetlands land cover classification and hyperspectral remote sensing. *Journal of Environmental Management*, 2009: 2170-2177.